Oncology Research, Vol. 26, pp. 1235–1243
Printed in the USA.

0965-0407/18 $90.00 + .00
DOI: https://doi.org/10.3727/096504018X15179661552702
E-ISSN 1555-3906
www.cognizantcommunication.com

Triptolide Inhibits Proliferation and Migration of Human Neuroblastoma SH-SY5Y Cells by Upregulating MicroRNA-181a

Jian Jiang,* Xuewen Song,† Jing Yang,* Ke Lei,* Yongan Ni,* Fei Zhou,‡ and Lirong Sun*

*Department of Pediatrics, The Affiliated Hospital of Qingdao University, Qingdao, Shandong, P.R. China
†Outpatient Department, Qingdao No. 1 Sanitarium, Qingdao, Shandong, P.R. China
‡Department of Oncology, The Affiliated Hospital of Qingdao University, Qingdao, Shandong, P.R. China

Neuroblastoma is the primary cause of cancer-related death for children 1 to 5 years of age. New therapeutic strategies and medicines are urgently needed. This study aimed to investigate the effects of triptolide (TPL), the major active component purified from *Tripterygium wilfordii* Hook F, on neuroblastoma SH-SY5Y cell proliferation, migration, and apoptosis, as well as underlying potential mechanisms. We found that TPL inhibited SH-SY5Y cell viability, proliferation, and migration, but induced cell apoptosis. The expression of matrix metalloproteinase-2 (MMP-2) and MMP-9 after TPL treatment in SH-SY5Y cells was decreased. The expression of microRNA-181a (miR-181a) was upregulated after TPL treatment. Moreover, suppression of miR-181a reversed the effects of TPL on SH-SY5Y cell proliferation, apoptosis, and migration. Overexpression of miR-181a enhanced the TPL-induced activation of p38 mitogen-activated protein kinase (p38MAPK) and nuclear factor κ light chain enhancer of activated B cells (NF-κB) pathways. In conclusion, our research verified that TPL inhibited the proliferation and migration of human neuroblastoma SH-SY5Y cells by upregulating the expression of miR-181a.

Key words: Triptolide; MicroRNA-181a; Neuroblastoma; Cell apoptosis; p38MAPK signaling pathway; NF-κB signaling pathway

INTRODUCTION

Neuroblastoma, a type of postganglionic sympathetic tumor, is the primary cause of cancer-related death for children between 1 and 5 years old[1,2]. The clinical symptoms of neuroblastoma are highly variable and dependent on several factors such as age of presentation, stage, ploidy, and genomic abnormalities[3,4]. Epidemiological data suggest that the incidence of neuroblastoma has remarkably increased in recent decades[2,5]. Surgical resection, chemotherapy, and radiotherapy only temporarily improve the clinical symptoms of neuroblastoma, but cannot inhibit neuroblastoma recurrence and metastasis completely[6,7]. Identifying new therapeutic strategies and medicines for the treatment of neuroblastoma is urgently needed.

Plant-derived medicines have attracted attention all over the world because of their potential safety, efficiency, and minimal side effects in cancer therapy[8,9]. Triptolide (TPL), a diterpenoid triexpoxide, is the major active component purified from *Tripterygium wilfordii* Hook F, which has been demonstrated to possess wide bioactivities such as anti-inflammatory[10], antioxidative[11], antirheumatoid[12], and antitumor[13,14]. Zhu et al. demonstrated that TPL inhibited the angiogenesis of anaplastic thyroid carcinoma by targeting vascular endothelial and tumor cells[15]. The experimental study from Huang et al. indicated that TPL suppressed the proliferation of prostate cancer cells by downregulating the expression of small ubiquitin-like modifier 1 (SUMO)-specific protease 1[16]. In terms of neuroblastoma, Yan et al. demonstrated that TPL inhibited the cell proliferation and tumorigenesis of human neuroblastoma[17]. Krosch et al. reported that the nuclear factor κ light chain enhancer of activated B cell (NF-κB) signaling pathway was involved in the TPL-induced neuroblastoma cell apoptosis and autophagy[18].

MicroRNAs (miRNAs) are small single-stranded RNAs in eukaryotic cells that participate in the regulation of cell proliferation, differentiation, and apoptosis by modulating the gene expression at the posttranscriptional level[19]. miRNA-181a (miR-181a) has been found to show tumor-suppressive effects against oral squamous cell

Address correspondence to Lirong Sun, Department of Pediatrics, The Affiliated Hospital of Qingdao University, No. 1677 Wutaishan Road, Huangdao District, Qingdao 266555, Shandong, P.R. China. Tel: +86-0532-82911847; E-mail: Sunlir1011@126.com

carcinoma[20] and gastric cancer HGC-27 cells[21], while presenting tumor-promotable effects in ovarian cancer[22] and colorectal cancer[23]. Cheng et al. reported that miR-181a suppressed parkin-mediated mitophagy and sensitized neuroblastoma cells to mitochondrial uncoupler-induced apoptosis[24]. More research is needed to further explore the effects of miR-181a on neuroblastoma cell apoptosis as well as the roles of miR-181a in TPL-induced neuroblastoma cell apoptosis.

Therefore, in the present study, we utilized the human neuroblastoma cell line SH-SY5Y to further validate the antitumor effects of TPL and to explore the effects of miR-181a on TPL-induced neuroblastoma cell proliferation inhibition and apoptosis. These findings will be helpful for understanding the critical roles of miR-181a in neuroblastoma cell proliferation and apoptosis and provide new therapeutic medicine for neuroblastoma therapy.

MATERIALS AND METHODS

Cell Culture

Human neuroblastoma SH-SY5Y cells were obtained from Stem Cell Bank, Chinese Academy of Science (Shanghai, P.R. China). Cells were cultured in Dulbecco's modified Eagle's medium (DMEM; Gibco, Life Technologies, Carlsbad, CA, USA) containing 10% fetal bovine serum (FBS; Gibco, Life Technologies), 100 U/ml penicillin–100 μg/ml streptomycin solutions (Hyclone, Logan, UT, USA), and 1 mM L-glutamine (Sigma-Aldrich, St. Louis, MO, USA). Cultures were maintained in a humidity incubator (Thermo Fisher Scientific, Waltham, MA, USA) at 37°C with 5% CO_2.

Preparation of TPL Solution

TPL was purchased from Sigma-Aldrich (T3652) and dissolved in dimethyl sulfoxide (DMSO; Sigma-Aldrich) to a storage concentration of 50 mM. TPL solution was sterilized through a 0.22-μm filter (Millipore, Bedford, MA, USA) and stored at −20°C according to the manufacturer's instruction. Serum-free DMEM was used to dilute TPL to 10, 20, or 50 nM before the experiments. The chemical structure of TPL is shown in Figure 1.

Evaluation of Cell Viability

Cell counting kit-8 (CCK-8; Beyotime Biotechnology, Shanghai, P.R. China) assay was performed to evaluate the viability of SH-SY5Y cells after different concentrations of TPL treatment. Briefly, 1×10^4 SH-SY5Y cells per well were seeded into a 96-well plate (Corning Incorporated, New York, NY, USA) and exposed to 10, 20, or 50 nM TPL treatment for 24 h. The CCK-8 solution (10 μl) was added to the culture medium of each well. After that, the cell plate was incubated in humidity incubator for 1 h at 37°C, and the absorbance of each well at 450 nm was recorded using a microplate reader (Bio-Tek, Winooski, VT, USA). Cell viability (%) was calculated as follows: average absorbance of TPL treatment group/average absorbance of DMSO group×100%.

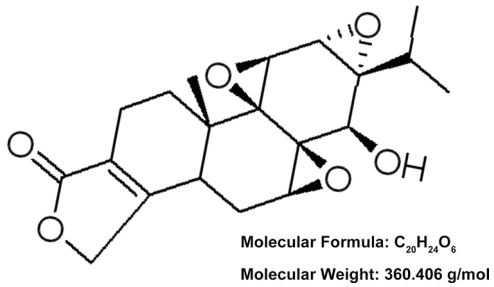

Figure 1. Chemical structure of triptolide (TPL).

Determination of Cell Proliferation

Cell proliferation was determined using a 5-bromo-2′-deoxyuridine (BrdU) incorporation assay kit (Sigma-Aldrich) following the manufacturer's instructions. Briefly, 3×10^4 SH-SY5Y cells per well were seeded into 24-well plates. BrdU solution was added into each well before 20 nM TPL treatment. After culturing for 24 h, the number of $BrdU^+$ cells of each group was counted, which was proportional to cell proliferation.

Analysis of Cell Apoptosis

Fluorescein isothiocynate (FITC)-conjugated annexin V and propidium iodide (PI) staining was performed to analyze the apoptosis of SH-SY5Y cells after relevant treatment. Briefly, 3×10^4 SH-SY5Y cells per well were seeded into 24-well plates and exposed to a different treatment for 24 h. The adherent and floating cells were both harvested and washed with phosphate-buffered saline (PBS) twice. Then the cells were diluted in 100 μl and incubated with 100 μl FITC-Annexin-V/ PI detection kit buffer (Yeasen, Shanghai, P.R. China) for 20 min at 37°C in the dark. Cell apoptosis was quantified using Guava easyCyte 8HT (Millipore) in line with the manufacturer's protocol.

Assessment of Cell Migration

Migration of SH-SY5Y cells was assessed using a two-chamber Transwell assay with a pore size of 8 mm. Briefly, 3×10^4 SH-SY5Y cells per well were seeded into 24-well plates and exposed to a different treatment for 24 h. Adherent cells were harvested and washed with PBS three times. Then 1×10^4 SH-SY5Y cells of each sample were resuspended in 200 μl of serum-free DMEM and added into the upper chamber. Complete DMEM (600 μl) was added into the lower chamber. After incubation at

37°C for 48 h, cells were immediately fixed with methanol. Nontraversed cells in the upper chamber were carefully removed using a cotton swab, and traversed cells in the lower chamber were counted under a microscope (Nikon, Japan). Relative migration (%) was calculated as follows: number of traversed cells in the treated group/number of traversed cells in the DMSO group×100%.

Quantitative Reverse Transcription PCR (qRT-PCR)

Total RNA in SH-SY5Y cells was isolated using TRIzol™ Plus RNA Purification Kit (Invitrogen, Carlsbad, CA, USA) according to the manufacturer's instruction. Single-stranded cDNA was synthesized using SuperScript™ IV First-Strand Synthesis System (Invitrogen). For the detection of the expression of miR-181a, SuperScript™ III Platinum™ One-Step qRT-PCR kit (Invitrogen) was used following the manufacturer's instruction. The primers for miR-181a were 5′-GCT GGCAACATTCAACGCTGTC-3′ (forward) and 5′-GT GCAGGGTCCGAGGT-3′ (reverse). U6 small nuclear RNA was used as an internal control. The primers for U6 were 5′-ATTGGAACGATACAGAGAAGAT-3′ (forward) and 5′-GGAACGCTTCACGAATTT-3′ (reverse). Data were calculated using the $2^{-\Delta\Delta Ct}$ method[25].

Cell Transfection

The sequences of miR-181a inhibitor, miR-181a mimic, and their negative controls (NC, Scramble) were synthesized by GenePharma (Shanghai, P.R. China). Cell transfection was performed using Lipofectamine 3000 reagent (Invitrogen) in line with the manufacturer's instruction. The transfection efficiency was verified using qRT-PCR.

Western Blotting

Total protein in SH-SY5Y cells after different treatments was isolated using RIPA lysis and extraction buffer (Thermo Fisher Scientific) according to the manufacturer's protocol. The concentrations of proteins were quantified using BCA™ Protein Assay Kit (Thermo Fisher Scientific). Western blotting system was established using the Bio-Rad Bis-Tris Gel System (Bio-Rad Laboratories, Hercules, CA, USA) in line with the manufacturer's instruction and performed as previously described[26]. Equal concentrations of proteins were electrophoresed and transferred onto nitrocellulose membranes (Millipore), which were incubated with relevant antibodies. All primary antibodies used in this study were purchased from Abcam Biotechnology (Cambridge, MA,

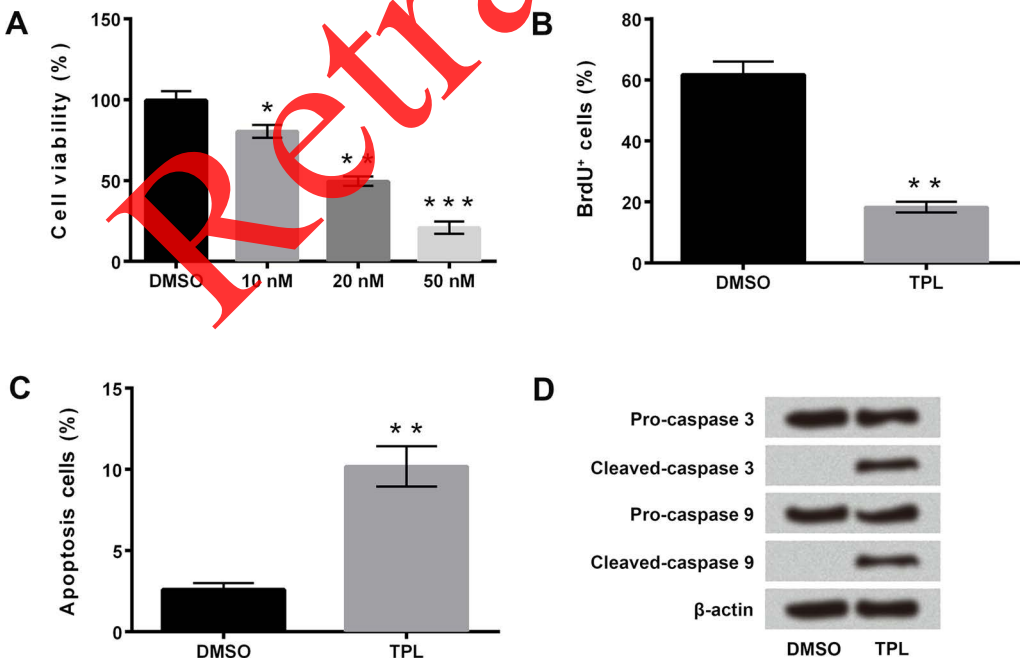

Figure 2. TPL inhibited proliferation and induced apoptosis of SH-SY5Y cells. (A) Viabilities of SH-SY5Y cells after 10, 20, or 50 nM TPL treatments were measured using cell counting kit-8 (CCK-8) assay. (B) Proliferation of SH-SY5Y cells after 20 nM TPL treatment was detected using 5-bromo-2′-deoxyuridine (BrdU) incorporation assay. (C) Fluorescein isothiocynate (FITC)-conjugated annexin V and propidium iodide (PI) staining was used to determine the SH-SY5Y cell apoptosis after 20 nM TPL treatment. (D) The expressions of caspase 3 and caspase 9 in SH-SY5Y cells after 20 nM TPL treatment were analyzed using Western blotting. Data are presented as the mean±standard deviation (SD). DMSO, dimethyl sulfoxide. *$p<0.05$, **$p<0.01$, ***$p<0.001$.

USA): anti-caspase 3 antibody (ab13585), anti-caspase 9 antibody (ab32539), anti-matrix metalloproteinase-2 (MMP-2) antibody (ab97779), anti-MMP-9 antibody (ab137867), anti-total (t)-p38MAPK antibody (ab27986), anti-phosphorylated (p)-p38-mitogen-activated protein kinase (MAPK) antibody (ab178867), anti-t-NF-κB subunit 1 (p65) antibody (ab32536), anti-p-p65 antibody (ab86299), anti-t-inhibitor of NF-κB-α (IκBα) antibody (ab32518), anti-p-IκBα antibody (ab133462), and anti-β-actin antibody (ab8227). Subsequently, the membranes were incubated with secondary antibodies {goat anti-rabbit (or anti-mouse) IgG H&L [horseradish peroxidase (HRP); ab205718 or ab205719; Abcam]} for 1 h at room temperature, followed by adding 200 µl of Immobilon Western Chemiluminescent HRP Substrate (Millipore) to the surface of membranes. The protein signals were recorded using the Bio-Rad ChemiDoc™ XRS system (Bio-Rad Laboratories). The protein expression was quantified using Image Lab™ Software (Bio-Rad Laboratories)[27].

Statistical Analysis

All experiments in this study were repeated at least three times. Results of multiple experiments were presented as the mean±standard deviation (SD). GraphPad 6.0 software (GraphPad, San Diego, CA, USA) was used for statistical analysis. The p values were calculated using one-way analysis of variance (ANOVA) or Student's t-test. A value of $p<0.05$ was considered statistically significant.

RESULTS

TPL Inhibited Proliferation and Induced Apoptosis of SH-SY5Y Cells

The effects of TPL on SH-SY5Y cell viability, proliferation, and apoptosis were detected using CCK-8 assay, BrdU incorporation assay, and FITC-annexin V/PI staining, respectively. As presented in Figure 2A, 10, 20, or 50 nM TPL treatments significantly inhibited the viability of the SH-SY5Y cells in a dose-dependent manner ($p<0.05$, $p<0.01$, or $p<0.001$). Considering that the IC_{50} value was calculated as 20.16 nM, 20 nM TPL was selected for further experiments. Figure 2B shows that the proportion of $BrdU^+$ cells was remarkably reduced after 20 nM TPL treatment ($p<0.01$), which displayed that TPL markedly inhibited the proliferation of SH-SY5Y cells. Moreover, the proportion of apoptotic cells was notably increased after 20 nM TPL treatment ($p<0.01$) (Fig. 2C). Western blotting showed that the expressions of cleaved caspase 3 and cleaved caspase 9 in SH-SY5Y cells after TPL treatment were noticeably enhanced (Fig. 2D). These above results suggested that TPL inhibited the proliferation and induced the apoptosis of SH-SY5Y cells.

TPL Inhibited the Migration of SH-SY5Y Cells

The effect of TPL on the migration of SH-SY5Y cells was measured using a two-chamber Transwell assay and Western blotting. Figure 3A shows that after 20 nM TPL treatment, the relative migration of SH-SY5Y cells was significantly decreased ($p<0.05$). In addition, as shown in Figure 3B, TPL treatment remarkably down-regulated the expression levels of MMP-2 and MMP-9 in SH-SY5Y cells ($p<0.05$ or $p<0.01$). These above findings indicated that TPL inhibited the migration of SH-SY5Y cells.

TPL Enhanced the Expression of miR-181a in SH-SY5Y Cells

The relative expression of miR-181a in SH-SY5Y cells after 20 nM TPL treatment was determined using qRT-PCR. Figure 4 reveals that 20 nM TPL treatment

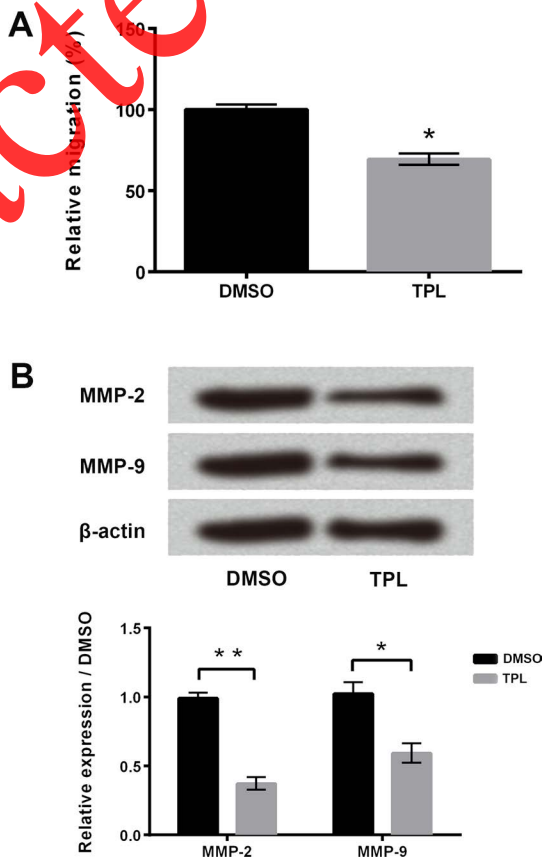

Figure 3. TPL inhibited the migration of SH-SY5Y cells. (A) Relative migration of SH-SY5Y cells after 20 nM TPL treatment was detected using two-chamber Transwell assay. (B) Western blotting was performed to analyze the expressions of matrix metalloproteinase-2 (MMP-2) and MMP-9 in SH-SY5Y cells after 20 nM TPL treatment. Data are presented as the mean±SD. *$p<0.05$, **$p<0.01$.

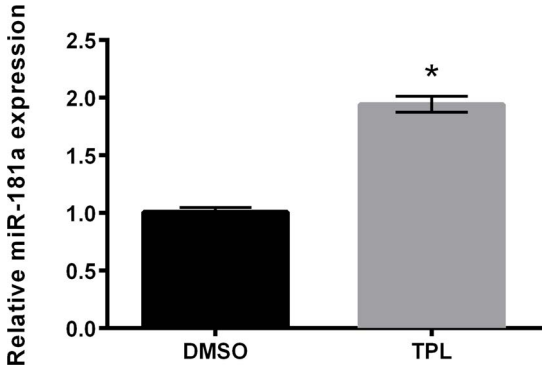

Figure 4. TPL enhanced the expression of microRNA-181a (miR-181a) in SH-SY5Y cells. Quantitative reverse transcription polymerase chain reaction (qRT-PCR) was used to measure the expression of miR-181a in SH-SY5Y cells after 20 nM TPL treatment. Data are presented as the mean ± SD. *$p < 0.05$.

obviously upregulated the expression level of miR-181a in SH-SY5Y cells ($p < 0.05$). This result suggested that miR-181a might participate in the effects of TPL on SH-SY5Y cell proliferation and apoptosis.

Suppression of miR-181a Reversed the Effects of TPL on SH-SY5Y Cell Proliferation, Apoptosis, and Migration

To further explore the effects of miR-181a on the TPL-induced SH-SY5Y cell proliferation and migration inhibition as well as apoptosis enhancement, miR-181a inhibitor or miR-181a mimic was transfected into SH-SY5Y cells, respectively. As presented in Figure 5A, the expression levels of miR-181a in SH-SY5Y cells were significantly decreased after miR-181a inhibitor transfection ($p < 0.01$) and remarkably increased after miR-181 mimic transfection ($p < 0.01$). Figure 5B indicates that compared to single TPL treatment, the proportion of $BrdU^+$ cells after TPL + miR-181a inhibitor treatment was remarkably increased ($p < 0.05$), which suggested that suppression of miR-181a significantly reversed the TPL-induced SH-SY5Y cell proliferation inhibition. Figure 5C shows that miR-181a inhibitor transfection markedly decreased the TPL-induced SH-SY5Y cell apoptosis ($p < 0.01$). The expression levels of cleaved caspase 3 and cleaved caspase 9 in SH-SY5Y cells after miR-181a inhibitor transfection were also reduced (Fig. 5D). In addition, results in Figure 5E show that compared to TPL treatment only, the relative migration of SH-SY5Y cells after TPL treatment and miR-181a transfection was significantly increased ($p < 0.05$). Western blotting revealed that the expressions of MMP-2 and MMP-9 in SH-SY5Y cells were obviously enhanced after TPL treatment and miR-181a inhibitor transfection, compared to single TPL treatment ($p < 0.05$) (Fig. 5F). These above findings suggested that miR-181a was involved in the effects of TPL on SH-SY5Y cell proliferation, apoptosis, and migration.

TPL Promoted the Activation of the p38MAPK and NF-κB Pathways in SH-SY5Y Cells

The effects of TPL and miR-181a on the activation of p38MAPK and NF-κB in SH-SY5Y cells were also investigated in our research. Figure 6A reveals that TPL single treatment obviously upregulated the expression of p-p38MAPK in SH-SY5Y cells, and miR-181a mimic transfection markedly enhanced the TPL-induced increase in p-p38MAPK ($p < 0.01$). Similar results were found in the NF-κB signaling pathway, which presented that the expressions of p-p65 and p-IκBα in SH-SY5Y cells were increased after single TPL treatment and were further upregulated after TPL treatment and miR-181a mimic transfection ($p < 0.01$) (Fig. 6B). These findings provided evidence that TPL promoted the activation of the p38MAPK and NF-κB signaling pathways in SH-SY5Y cells.

DISCUSSION

Neuroblastoma remains a therapeutic challenge for researchers because of the occurrence of tumor recurrence and metastasis after surgical resection, chemotherapy, and radiotherapy[28]. This study revealed that TPL, a compound isolated from *Tripterygium wilfordii* Hook F, distinctly inhibited neuroblastoma SH-SY5Y cell proliferation and migration but remarkably promoted cell apoptosis. Moreover, the expression of miR-181a was increased after TPL treatment. Suppression of miR-181a obviously reversed the TPL-induced SH-SY5Y cell proliferation and migration inhibition, as well as apoptosis enhancement. Overexpression of miR-181a enhanced the TPL-induced activation of the p38MAPK and NF-κB pathways in SH-SY5Y cells.

Cell apoptosis plays critical roles in maintaining homeostasis and can be induced and regulated by many intracellular and extracellular molecules[29,30]. Inducing cancer cell apoptosis is considered to be the most effective method for cancer therapy[31]. Previous studies have demonstrated the antitumor effects of TPL on neuroblastoma[17,18]. In this study, we also found that TPL inhibited the viability and proliferation of SH-SY5Y cells in a dose-dependent manner. Moreover, TPL induced SH-SY5Y cell apoptosis by upregulating the expressions of cleaved caspase 3 and cleaved caspase 9. These findings further proved the anticancer effects of TPL on neuroblastoma.

Inhibition of tumor metastasis is also considered as the important purpose in neuroblastoma treatment[32]. In the process of neuroblastoma metastasis, neuroblastoma cells obtain migration and invasion abilities to spread from the primary tumor site and establish secondary

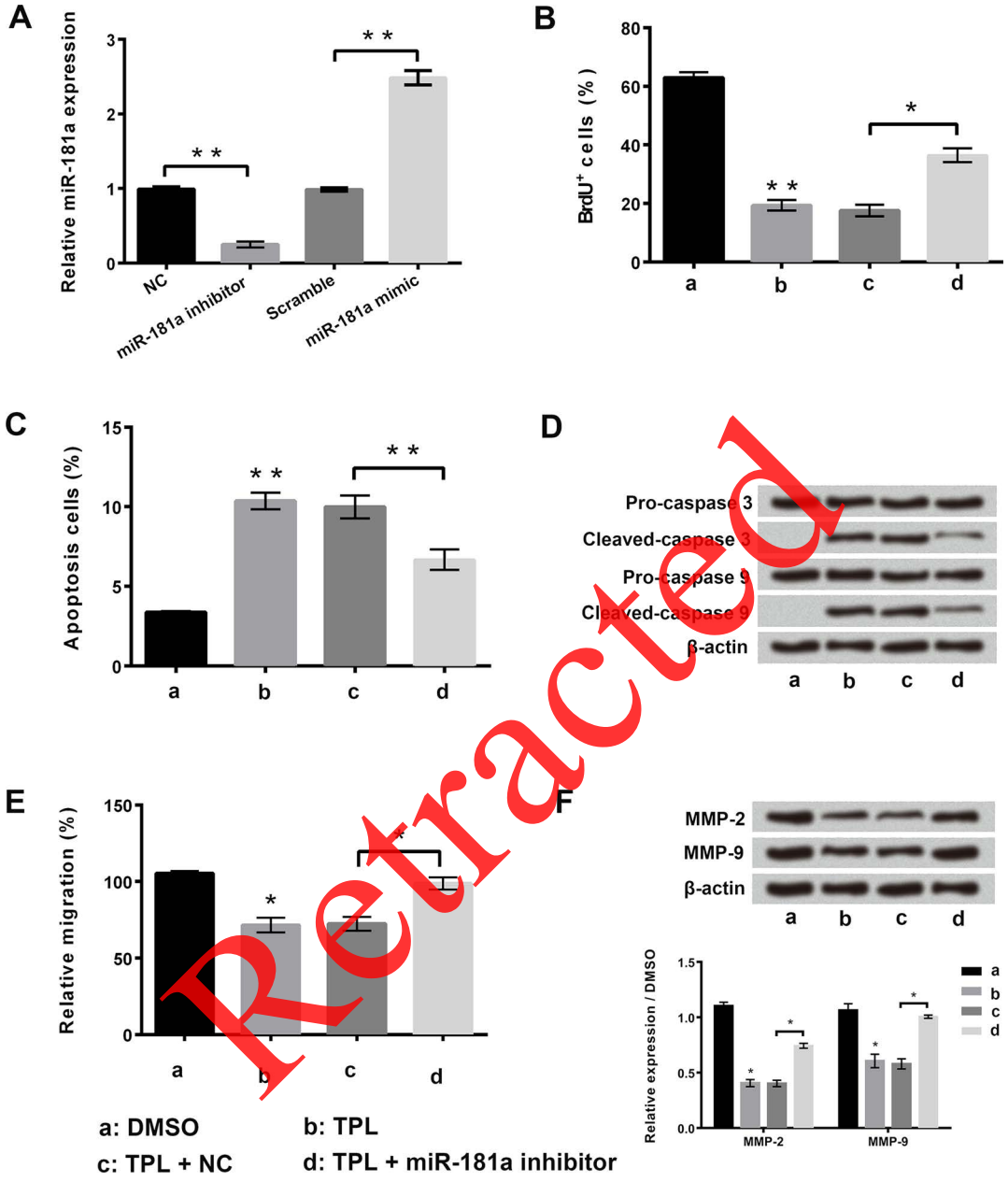

Figure 5. Suppression of miR-181a reversed the effects of TPL on SH-SY5Y cell proliferation, apoptosis, and migration. (A) qRT-PCR was performed to detect the expressions of miR-181a in SH-SY5Y cells after negative control (NC), miR-181a inhibitor, or miR-181a mimic transfection. (B) Proliferation and (C) apoptosis of SH-SY5Y cells after TPL treatment and/or miR-181a inhibitor transfection were measured using BrdU incorporation assay and FITC-conjugated annexin V and PI staining, respectively. (D) Western blotting was used to analyze the expression levels of caspase 3 and caspase 9 in SH-SY5Y cells after TPL treatment and/or miR-181a inhibitor transfection. (E) Relative migration of SH-SY5Y cells after TPL treatment and/or miR-181a inhibitor transfection was detected using two-chamber Transwell assay. (F) The expressions of MMP-2 and MMP-9 in SH-SY5Y cells after TPL treatment and/or miR-181a inhibitor transfection were analyzed using Western blotting. Data are presented as the mean±SD. *$p<0.05$, **$p<0.01$.

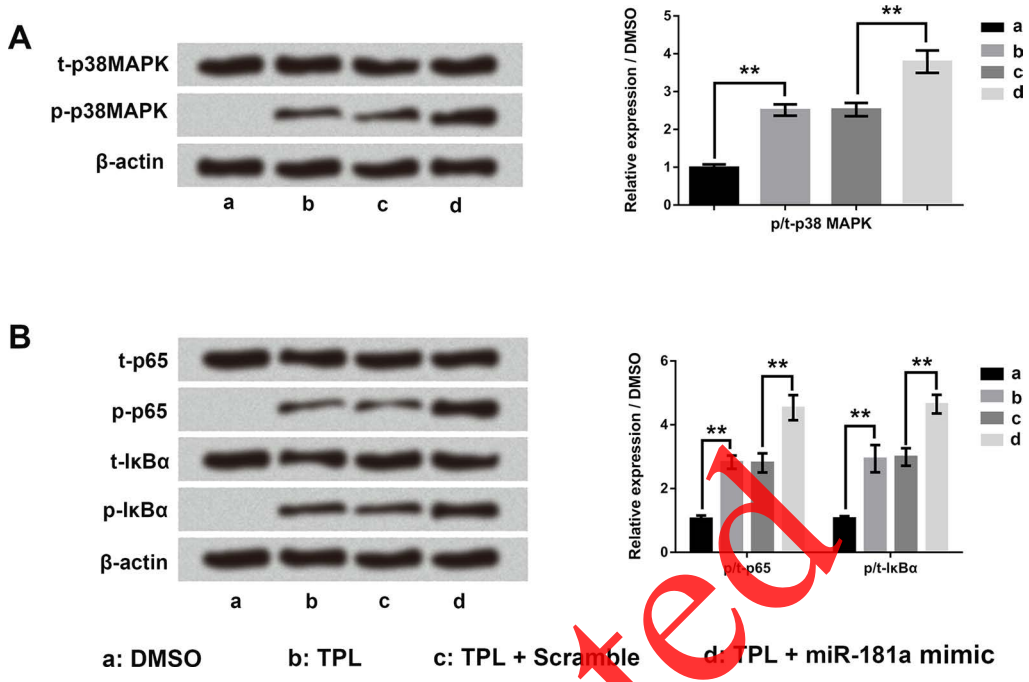

Figure 6. TPL promoted the activation of the p38 mitogen-activated protein kinase (p38MAPK) and nuclear factor κ light chain enhancer of activated B cells (NF-κB) pathway in SH-SY5Y cells. (A, B) Western blotting was used to analyze the expressions of p38MAPK, NF-κB subunit 1 (p65), and NF-κB inhibitor α (IκBα) in SH-SY5Y cells after TPL treatment and/or miR-181a mimic transfection. Data are presented as the mean±standard deviation (SD). $^{**}p<0.01$.

tumors at other sites[33]. MMPs, especially MMP-2 and MMP-9, have been shown to participate in the tumor cell migration and invasion through various signal transduction pathways[34]. In our experiments, the relative migration of SH-SY5Y cells and the expressions of MMP-2 and MMP-9 in SH-SY5Y cells after TPL treatment were both decreased, which revealed that TPL also had anticancer effects on neuroblastoma by inhibiting neuroblastoma cell migration.

miRNAs do not encode proteins, but they regulate intracellular gene expression at the posttranscriptional level[35]. Research has demonstrated that miR-181a has various effects on different tumor cells[20–23]. In the present study, we found that miR-181a was upregulated after TPL treatment in SH-SY5Y cells. Suppression of miR-181a significantly reversed the TPL-induced SH-SY5Y cell proliferation and migration inhibition, as well as apoptosis enhancement. These above findings suggested that miR-181a showed a tumor-suppressive effect against SH-SY5Y cells and was involved in the effects of TPL on SH-SY5Y cell proliferation, migration, and apoptosis. Moreover, these results were consistent with the previous study, which pointed out that miR-181a showed tumor-suppressive effects against oral squamous cell carcinoma and gastric cancer HGC-27 cells[20,21].

Numerous studies have demonstrated that the p38MAPK and NF-κB signaling pathways play important roles in the regulation of various cancer cell functions, such as proliferation, differentiation, migration, autophagy, and apoptosis[36,37]. Dedoni et al. reported that interferon-β counter-induced human neuroblastoma SH-SY5Y cell apoptosis by activating the p38MAPK signaling pathway[38]. Liu et al. demonstrated that 7,8-dihydroxycoumarins protected human neuroblastoma cells from Aβ-induced neurotoxic damage through inhibiting the C-jun N-terminal kinase 1 (JNK) and p38MAPK signaling pathways[39]. Song et al. pointed out that chrysotoxine, a bibenzyl compound, inhibited 6-hydroxydopamine-mediated SH-SY5Y cell apoptosis via mitochondria protection and NF-κB modulation[40]. In this study, we also explored the effects of TPL and miR-181a on the p38MAPK and NF-κB signaling pathways in SH-SY5Y cells. We found that TPL single treatment activated the p38MAPK and NF-κB signaling pathways in SH-SY5Y cells by upregulating the expressions of p-p38MAPK, p-p65, and p-IκBα. In addition, overexpression of miR-181a obviously enhanced TPL-induced activation of p38MAPK and NF-κB signaling pathways in SH-SY5Y cells through further increasing the expression levels of p-p38MAPK, p-p65, and p-IκBα. These findings imply that the p38MAPK and NF-κB signaling pathways may participate in the effects of TPL and miR-181a on SH-SY5Y cells, although the specific cellular mechanisms are unknown.

In conclusion, our research verified that TPL inhibited the proliferation and migration of human neuroblastoma SH-SY5Y cells by upregulating the expression of miR-181a. We proposed that TPL could be an effective therapeutic medicine for neuroblastoma treatment, despite further in vivo study and safety evaluation are still needed.

ACKNOWLEDGMENT: This work was not supported by any funding agency. The authors declare no conflicts of interest.

REFERENCES

1. van Engelen K, Merks JH, Lam J, Kremer LC, Backes M, Baars MJ, van der Pal HJ, Postma AV, Versteeg R, Caron HN, Mulder BJ. Prevalence of congenital heart defects in neuroblastoma patients: A cohort study and systematic review of literature. Eur J Pediatr. 2009;168(9):1081–90.
2. Louis CU, Shohet JM. Neuroblastoma: Molecular pathogenesis and therapy. Annu Rev Med. 2015;66:49–63.
3. Welch C, Chen Y, Stallings RL. MicroRNA-34a functions as a potential tumor suppressor by inducing apoptosis in neuroblastoma cells. Oncogene 2007;26(34):5017–22.
4. Chen QR, Song YK, Yu LR, Wei JS, Chung JY, Hewitt SM, Veenstra TD, Khan J. Global genomic and proteomic analysis identifies biological pathways related to high-risk neuroblastoma. J Proteome Res. 2010;9(1):373–82.
5. Kamihara J, Ma C, Fuentes Alabi SL, Garrido C, Frazier AL, Rodriguez-Galindo C, Orjuela MA. Socioeconomic status and global variations in the incidence of neuroblastoma: Call for support of population-based cancer registries in low-middle-income countries. Pediatr Blood Cancer 2017;64(2):321–3.
6. Shirzadi AS, Drazin DG, Strickland AS, Bannykh SI, Johnson JP. Vertebral column metastases from an esthesioneuroblastoma: Chemotherapy, radiation, and resection for recurrence with 15-year followup. Case Rep Surg. 2013;2013:107315.
7. Venat-Bouvet L, Le Brun-Ly V, Martin J, Gasnier O, Falkowsky S, Tubiana-Mathieu N. Long-term survival in adult neuroblastoma with multiple recurrences. Case Rep Oncol. 2010;3(1):45–8.
8. Cragg GM, Newman DJ. Plants as a source of anti-cancer agents. J Ethnopharmacol. 2005;100(1–2):72–9.
9. Yan H, Wang X, Niu J, Wang Y, Wang P, Liu Q. Anticancer effect and the underlying mechanisms of gypenosides on human colorectal cancer SW-480 cells. PLoS One 2014;9(4):e95609.
10. Wang X, Zhang L, Duan W, Liu B, Gong P, Ding Y, Wu X. Anti-inflammatory effects of triptolide by inhibiting the NF-kappaB signalling pathway in LPS-induced acute lung injury in a murine model. Mol Med Rep. 2014;10(1):447–52.
11. Yu H, Shi L, Zhao S, Sun Y, Gao Y, Sun Y, Qi G. Triptolide attenuates myocardial ischemia/reperfusion injuries in rats by inducing the activation of Nrf2/HO-1 defense pathway. Cardiovasc Toxicol. 2016;16(4):325–35.
12. Jiang J, Wang N, Guan Z, Houshan LV. Programmed cell death 5 factor enhances triptolide-induced fibroblast-like synoviocyte apoptosis of rheumatoid arthritis. Artif Cells Blood Substit Immobil Biotechnol. 2010;38(1):38–42.
13. Westfall SD, Nilsson EE, Skinner MK. Role of triptolide as an adjunct chemotherapy for ovarian cancer. Chemotherapy 2008;54(1):67–76.
14. Chen YW, Lin GJ, Chia WT, Lin CK, Chuang YP, Sytwu HK. Triptolide exerts anti-tumor effect on oral cancer and KB cells in vitro and in vivo. Oral Oncol. 2009;45(7):562–8.
15. Zhu W, He S, Li Y, Qiu P, Shu M, Ou Y, Zhou Y, Leng T, Xie J, Zheng X, Xu D, Su X, Yan G. Anti-angiogenic activity of triptolide in anaplastic thyroid carcinoma is mediated by targeting vascular endothelial and tumor cells. Vascul Pharmacol. 2010;52(1–2):46–54.
16. Huang W, He T, Chai C, Yang Y, Zheng Y, Zhou P, Qiao X, Zhang B, Liu Z, Wang J, Shi C, Lei L, Gao K, Li H, Zhong S, Yao L, Huang ME, Lei M. Triptolide inhibits the proliferation of prostate cancer cells and down-regulates SUMO-specific protease 1 expression. PLoS One 2012;7(5):e37693.
17. Yan X, Ke XX, Zhao H, Huang M, Hu R, Cui H. Triptolide inhibits cell proliferation and tumorigenicity of human neuroblastoma cells. Mol Med Rep. 2015;11(2):791–6.
18. Krosch TC, Sangwan V, Banerjee S, Mujumdar N, Dudeja V, Saluja AK, Vickers SM. Triptolide-mediated cell death in neuroblastoma occurs by both apoptosis and autophagy pathways and results in inhibition of nuclear factor-kappa B activity. Am J Surg. 2013;205(4):387–96.
19. Liu J, Wu CP, Lu BF, Jiang JT. Mechanism of T cell regulation by microRNAs. Cancer Biol Med. 2013;10(3):131–7.
20. Sun KH, Bae SD, Hong HS, Kim RH, Kang MK, Park NH. miR-181a shows tumor suppressive effect against oral squamous cell carcinoma cells by downregulating K-ras. Biochem Biophys Res Commun. 2011;404(4):896–902.
21. Lin F, Li Y, Yan S, Liu S, Qian W, Shen D, Lin Q, Mao W. MicroRNA-181a inhibits tumor proliferation, invasiveness, and metastasis and is downregulated in gastric cancer. Oncol Res. 2015;22(2):75–84.
22. Parikh A, Lee C, Joseph P, Marchini S, Baccarini A, Kolev V, Romualdi C, Fruscio R, Shah H, Wang F, Mullokandov G, Fishman D, D'Incalci M, Rahaman J, Kalir T, Redline RW, Brown BD, Narla G, DiFeo A. microRNA-181a has a critical role in ovarian cancer progression through the regulation of the epithelial-mesenchymal transition. Nat Commun. 2014;5:2977.
23. Ji D, Chen Z, Li M, Zhan T, Yao Y, Zhang Z, Xi J, Yan L, Gu J. MicroRNA-181a promotes tumor growth and liver metastasis in colorectal cancer by targeting the tumor suppressor WIF-1. Mol Cancer 2014;13:86.
24. Cheng M, Liu L, Lao Y, Liao W, Liao M, Luo X, Wu J, Xie W, Zhang Y, Xu N. MicroRNA-181a suppresses parkin-mediated mitophagy and sensitizes neuroblastoma cells to mitochondrial uncoupler-induced apoptosis. Oncotarget 2016;7(27):42274–87.
25. Ish-Shalom S, Lichter A. Analysis of fungal gene expression by real time quantitative PCR. Methods Mol Biol. 2010;638:103–14.
26. Li R, Yin F, Guo YY, Zhao KC, Ruan Q, Qi YM. Knockdown of ANRIL aggravates H2O2-induced injury in PC-12 cells by targeting microRNA-125a. Biomed Pharmacother. 2017;92:952–61.
27. Nandi SS, Duryee MJ, Shahshahan HR, Thiele GM, Anderson DR, Mishra PK. Induction of autophagy markers is associated with attenuation of miR-133a in diabetic heart failure patients undergoing mechanical unloading. Am J Transl Res. 2015;7(4):683–96.
28. Buohliqa L, Upadhyay S, Nicolai P, Cavalieri R, Dolci RL, Prevedello D, Carrau RL. Possible esthesioneuroblastoma

metastasis to paranasal sinuses: Clinical report and literature review. Head Neck 2016;38(2):E32–6.
29. Yu SP. Regulation and critical role of potassium homeostasis in apoptosis. Prog Neurobiol. 2003;70(4):363–86.
30. Banerjee K, Ganguly A, Chakraborty P, Sarkar A, Singh S, Chatterjee M, Bhattacharya S, Choudhuri SK. ROS and RNS induced apoptosis through p53 and iNOS mediated pathway by a dibasic hydroxamic acid molecule in leukemia cells. Eur J Pharm Sci. 2014;52:146–64.
31. Xu H, Li X, Ding W, Zeng X, Kong H, Wang H, Xie W. Deguelin induces the apoptosis of lung cancer cells through regulating a ROS driven Akt pathway. Cancer Cell Int. 2015;15:25.
32. Zhang L, Yeger H, Das B, Irwin MS, Baruchel S. Tissue microenvironment modulates CXCR4 expression and tumor metastasis in neuroblastoma. Neoplasia 2007;9(1):36–46.
33. Kauffman EC, Robinson VL, Stadler WM, Sokoloff MH, Rinker-Schaeffer CW. Metastasis suppression: The evolving role of metastasis suppressor genes for regulating cancer cell growth at the secondary site. J Urol. 2003;169(3): 1122–33.
34. Gao Y, Guan Z, Chen J, Xie H, Yang Z, Fan J, Wang X, Li L. CXCL5/CXCR2 axis promotes bladder cancer cell migration and invasion by activating PI3K/AKT-induced upregulation of MMP2/MMP9. Int J Oncol. 2015;47(2): 690–700.
35. Salaun B, Yamamoto T, Badran B, Tsunetsugu-Yokota Y, Roux A, Baitsch L, Rouas R, Fayyad-Kazan H, Baumgaertner P, Devevre E, Ramesh A, Braun M, Speiser D, Autran B, Martiat P, Appay V, Romero P. Differentiation associated regulation of microRNA expression in vivo in human CD8+ T cell subsets. J Transl Med. 2011;9:44.
36. Cuenda A, Rousseau S. p38 MAP-kinases pathway regulation, function and role in human diseases. Biochim Biophys Acta 2007;1773(8):1358–75.
37. Nosrati N, Bakovic M, Paliyath G. Molecular mechanisms and pathways as targets for cancer prevention and progression with dietary compounds. Int J Mol Sci. 2017; 18(10):E2050.
38. Dedoni S, Olianas MC, Onali P. Interferon-beta counterregulates its own pro-apoptotic action by activating p38 MAPK signalling in human SH-SY5Y neuroblastoma cells. Apoptosis 2014;19(10):1509–26.
39. Liu GM, Xu X, Li J, Luo YG. 7,8-dithydroxycoumarins protect human neuroblastoma cells from Aβ- mediated neurotoxic damage via inhibiting JNK and p38MAPK pathways. Biomed Res. 2016;27(3):591–5.
40. Song JX, Shaw PC, Sze CW, Tong Y, Yao XS, Ng TB, Zhang YB. Chrysotoxine, a novel bibenzyl compound, inhibits 6-hydroxydopamine induced apoptosis in SH-SY5Y cells via mitochondria protection and NF-kappaB modulation. Neurochem Int. 2010;57(6):676–89.